Study of biological activity and targeted distribution of catesbeianalectin in mouse tissue

Rui-Li Zhao[#], Lin Zhu[#], Meng-Yue Liu, Tian-Ming Jin, Ji-Fei Ma*, Ye Hu, Xuan Wang, Shun-Yi Qin and Jian-Bao Chen

College of Animal Science and Veterinary Medicine, Tianjin Agriculture University, Tianjin, China

Abstract: Lectin has attracted attention because of its ability to serve as a carrier for targeted drug delivery. Large lectins isolated from marine invertebrates and crustaceans have strong immunogenicity and adverse effects, which limit their usefulness. This study reports the identification of catesbeianalectin via screening a bullfrog skin cDNA library. The catesbeianalectin polypeptide has a molecular weight of 1.47 kD, making it the smallest known lectin in terms of molecular weight. Circular dichroism analysis showed a PPII helix secondary structure. Catesbeianalectin strongly induces agglutination of rabbit erythrocytes and a variety of pathogens include *Staphylococcus aureus*, *Streptococcus suis* type 2, *Actinobacillus pleuropneumoniae*, and piglet paratyphoid *Salmonella*. The mean serum titer in catesbeianalectin-immunized Balb/c mice was 1:25, which was significantly lower than that of positive controls immunized with wheat germ agglutinin. Surface plasmon resonance indicated an S-type lectin. ^{125}I-labeled catesbeianalectin did not pass the blood-brain barrier. This study provides a basis for further research on the potential of catesbeianalectin as a carrier in targeted drug delivery.

Keywords: Catesbeianalectin, circular dichroism, immunogenicity, surface plasmon resonance imaging, ^{125}I-labeled

INTRODUCTION

Drugs and carriers that produce good therapeutic effects with low toxicity are the focus of significant effort in the fields of drug research and development (Yang *et al.,* 2015; Li *et al.,* 2013). In particular, resistance to antibiotics and the side effects of chemotherapy drugs used to treat patients with cancer are significant obstacles to effective treatment (Lehr and Gabor 2004; Jemal *et al.,* 2003). In recent years, more attention has been focused on biologically active peptides with anti-bacterial, anti-viral, and anti-cancer effects (Lehr 2000). Among biologically active polypeptides, lectins have been widely studied as second-generation bio-adhesive materials and targeted drug carriers because of the following characteristics: ability to agglutinate red blood cells and specifically bind with glycoproteins and sugar chains; small molecular weight; low toxicity; potent activity; good ability to penetrate the tumor cell membrane; high glycoprotein binding rate; capacity to improve drug loading while protecting the drug; and decreasing the dose delivered to non-target sites (Lehr 2000; Li *et al.,* 2008).

Early research on lectins was mainly focused on lectins from higher plants. In the late 1970s, research progressed to lectins from marine organisms. Lectins from a number of marine mollusks (Vasta *et al.,* 2011), crustaceans, spiders (Jiang *et al.,* 2009), and the skin of amphibians (Li *et al.,* 2008) have been purified and subjected to amino acid sequencing. In addition, the molecular structures, agglutinating effects, and biological functions of lectins from animal sources have been studied. For example, studies assessing odorranalectin from the skin of *Odorrana grahami* have shown that it is a mature peptide of 17 amino acids that could be used as a carrier in targeted drug delivery (Li *et al.,* 2008).

Catesbeianalectin, the focus of the present study, was screened from a bullfrog skin cDNA library and represents the first lectin obtained from bullfrog skin. The mature catesbeianalectin peptide has molecular weight of 1.47 kD and contains 13 amino acids. The biological activity and *in vivo* distribution of bullfrog catesbeianalectin have not been reported. Therefore, in the present study we determined the biological activity of catesbeianalectin, observed its agglutinating effect on common clinical pathogens via laser confocal microscopy, determined its secondary structure using circular dichroism (CD) technology, and screened more than 30 glycosylated ligands specifically bound with catesbeianalectin using surface plasmon resonance imaging (SPRi) technology. In addition, we carried out ^{125}I-labeling, serum stability analysis, and studies of the metabolism and targeting characteristics of catesbeianalectin in mouse tissue. The results of the present study provide an empirical basis for further research assessing the therapeutic potential of catesbeianalectin.

MATERIALS AND METHODS

Polypeptide synthesis

Catesbeianalectin was synthesized by Hongtuo Biological Technology Co., Ltd. (Zhejing, China) using solid phase

**Corresponding author:* e-mail: zhaoruili1109@126.com

peptide synthesis (SPPS) technology. Catesbeianalectin was desalted and purified using HPLC (Waters 600 controller, San Francisco, CA, USA) and reverse-phase C18 column chromatography. The molecular weight of catesbeianalectin was determined using fast atom bombardment mass spectrometry (FAB-MS, AB3200) (purity ≥95%).

Determination of the structure of catesbeianalectin

A circular dichroism (CD) spectrometer (Jasco-810, JASCO Corporation, Japan) was used to determine the structure of catesbeianalectin. CD spectral analysis was performed using CD Tool data processing software. The resulting data were subjected to online secondary structure analysis (http://dichroweb.cryst.bbk.ac.uk).

Determination of the agglutinating activity of catesbeianalectin

Rabbit erythrocytes were added to TBS-Ca^{2+} buffer and subjected to centrifugation at 1500-2000 rpm for 5-10 min. The erythrocytes were diluted, after which 10 μL of washed erythrocytes was added to 1mL of TBS-Ca^{2+} buffer. The erythrocyte suspension was added to a 96-well plate (40-45μL per well) with 5-10μL of the catesbeianalectin sample dissolved in saline. Observations were made after 45–60 min.

Serial dilution was used to dilute catesbeianalectin to different concentrations with saline. A bacterial suspension was prepared. The catesbeianalectin solution (25 μL) was mixed with 25μL of the bacterial suspension to be tested in a 500-μL centrifuge tube, which was kept at room temperature for 45 min. Finally, the solution was mixed and placed on a clean glass slide to allow observation of bacterial agglutination using a laser confocal microscope.

Determination of immunogenicity with catesbeianalectin

Specific pathogen-free Balb/c mice (n=24, 20±1 g) were randomly divided into four groups (6 mice/group): an ovalbumin (OVA) group, wheat germ agglutinin (WGA) group, catesbeianalectin group, and PBS control group. Catesbeianalectin (200μg/mL), WGA, and OVA were mixed with equal volumes of Freund's complete adjuvant and Freund's incomplete adjuvant for emulsion. The test compounds were administered by intraperitoneal injection (40 μg/mouse). After the first immunization, subsequent immunizations were made every 10 d. One week after the third immunization, a booster immunization was performed. Blood was collected 3–4 days after the booster immunization. Routine blood examinations and serum titer detections were performed, after which immunogenicity was determined.

In vitro screening of glycosylated ligands specific to catesbeianalectin

First, the sample glycan chip was fixed. The 3D chip was placed in EDC (Ethane Double Chlorine) (0.4 M)/NHS (N-hydroxysuccinimide) (0.1M) activation solution at room temperature for 30 min, washed with ultra-pure water, and dried with nitrogen gas. Next, 8-10μL of photocrosslinker was added to the chip and evenly covered by TADs (Reduced Glutathione). The reaction was allowed to proceed in the dark for 4 h at room temperature. The chip was washed with 3 times with EtOH (Ethyl alcohol), washed once with DMF (Dimethyl Formamide), and allowed to sit for 1 h. Equal volumes of DMSO (Dimethyl Sulphoxide) and PBS (Phosphate Buffer Saline) were mixed and used to produce a 10mM polysaccharide solution, which was added to a 96-well plate (200μL), which was placed in a instrument (BIODOT AD1500). After the sample was dried, the chip was placed in UV cross-linking equipment for 10 minutes (365nm, 1J/cm3), after which it was cleaned ultrasonically. An SPRi sensor was used to evaluate chip fixing.

The interaction between catesbeianalectin and sugar molecules was observed using SPRi equipment. PlexArray™ HT software was used to control the SPRi device. SPR detection software was used for real-time monitoring of the interaction between catesbeianalectin and sugar molecules.

^{125}I-catesbeianalectin preparation and radiochemical purity determination

The chloramine-T synthesis method was used to synthesize ^{125}I-catesbeianalectin. A Sephadex G-25 column was used to isolate and purify ^{125}I-catesbeianalectin. A radioactive TLC scanner was used to detect markers and assess radiochemical purity following purification (Gao *et al.,* 2013).

^{125}I-catesbeianalectin stability determination

Purified ^{125}I-catesbeianalectin (50μL) was added to 100 μL of PBS buffer and 100μL mouse serum. After mixing, the resulting solution was placed in a 37°C electric-heating type thermostatic water tank. After labeling for 10 min, 0.5h, 1h, 2h, 4h, and 6 h, radiochemical purity was determined (Gao *et al.,* 2013).

^{125}I-catesbeianalectin distribution in mouse tissue

Female ICR mice (SPF grade) weighing 20 ± 1 g were used for the drug metabolism experiment. The mice were divided into three groups based on the mode of administration: an intravenous (iv) injection group, intraperitoneal (ip) injection group, and intragastric (ig) administration group. The drug was administered at a dose of 2 mg/kg (5μCi/mouse). After drug administration, the mice were anesthetized for continuous in vivo imaging observation. The specific distribution of the drug was determined according to metabolic characteristics and time (Gao *et al.,* 2013).

Female ICR mice (6 weeks of age, n = 72, 20 ± 1 g) were used for the tissue distribution experiment. The mice were

divided into three groups based on the mode of administration: an intravenous (iv) injection group, intraperitoneal (ip) injection group, and intragastric (ig) administration group. The drug was administered at a dose of 5μCi/mouse. Four mice in each group were sacrificed 10min, 0.5h, 1h, 2h, 4h and 6h after drug administration. The heart, liver, spleen, lung, kidney, stomach, brain, and a blood sample were taken and weighed. Tissue radioactivity was determined using a γ counter and used to calculate cpm/g values, which were used to plot the metabolic curve.

All animal experiments were conducted in accordance with the guidelines of Tianjin Municipality on the Review of Welfare and Ethics of Laboratory Animals.

STATISTICAL ANALYSIS

The results of the experiments are expressed as mean ± SD. The significance of intra-group and inter-group differences was subjected to t-test analysis using SPSS19.0 software (IBM Corp., Armonk, NY, USA).

RESULTS

Catesbeianalectin synthesis

Using bullfrog skin cDNA library screening (Zhao *et al.*, 2009), we obtained the cDNA sequence of the catesbeianalectin precursor, which consists of 330 nucleotides. The mature catesbeianalectin peptide sequence contains 13 amino acids (FLTFPGMTFGKLL). This is the first report of a lectin obtained from bullfrog skin (fig. 1).

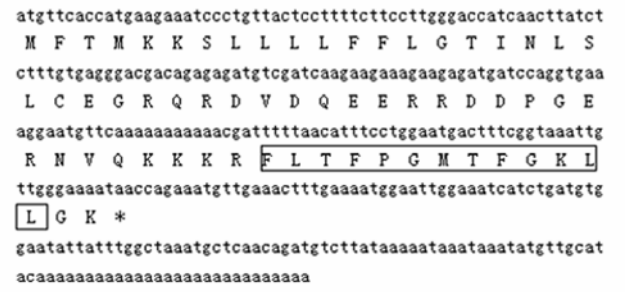

Fig. 1: cDNA sequence and amino acid sequence of the catesbeianalectin precursor (*termination codon)

Determination of the secondary structure of catesbeianalectin by CD

Catesbeianalectin in aqueous solution has a typical poly-proline type 2 (PPII) helical structure (see fig. 2).

Determination of the agglutinating activity of catesbeianalectin

The rabbit hemagglutination assay showed that catesbeianalectin caused hemagglutination (fig. 3). The minimum concentration of catesbeianalectin that produced agglutination was 6μg/mL.

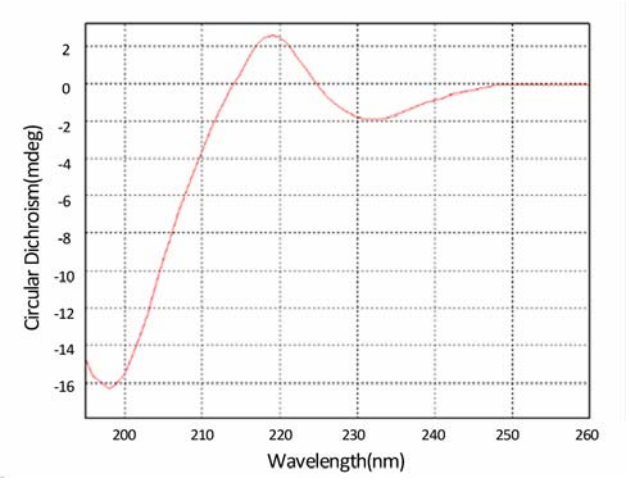

Fig. 2: CD spectrum of catesbeianalectin

Laser confocal microscopy was used to assess bacterial agglutination of *Staphylococcus aureus* (ATCC25923), *Streptococcus suis* type 2 (CVCC606), *Actinobacillus pleuropneumoniae* (CVCC259), and piglet paratyphoid *Salmonella* (S.C500) induced by catesbeianalectin. The minimum concentrations of catesbeianalectin that caused bacterial agglutination of *Staphylococcus aureus* (ATCC25923), *Streptococcus suis* type 2 (CVCC606), *Actinobacillus pleuropneumoniae* (CVCC259), and piglet paratyphoid *Salmonella* were 10 μg/mL, 5 μg/mL, 12.5 μg/mL, and 12.5 μg/mL, respectively (fig. 4). After exposure to the 4-fold MIC of catesbeianalectin, *Staphylococcus aureus* and *Actinobacillus pleuropneumoniae* were gathered into cell clusters of different sizes; *Streptococcus suis* type 2 and piglet paratyphoid *Salmonella* also obviously agglutinated.

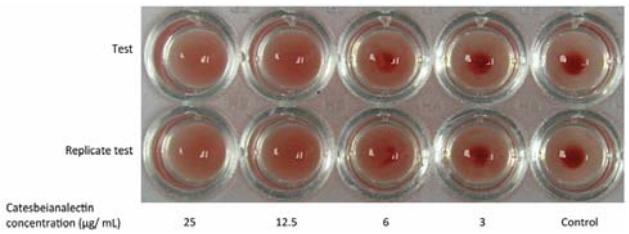

Fig. 3: Hemagglutination activity of catesbeianalectin

Determination of immunogenicity with catesbeianalectin

Mice immunized with OVA, WGA, catesbeianalectin, and vehicle were assessed. ELISA showed that the mean serum titer in mice was 1:200 at an OVA coating concentration of 0.25μg/mL. At a WGA coating concentration of 0.0078μg/mL, the mean serum titer in mice was 1:1600. At a catesbeianalectin coating concentration of 80μg/mL, the mean serum titer in mice was 1:25 (tables 1-3).

Screening of specific glycosylated ligands

Concanavalin A (ConA) was used as a positive control at a final concentration of 0.1mg/mL in diluted Hepes buffer

(pH 7.4). ConA had significant selectivity for the on-chip glucose and mannose sample points (see fig. 5). Catesbeianalectin at 0.4mg/mL had significant binding activity with galactoses and galactose-based polysaccharides (N-acetylgalactosamine) (See fig. 6).

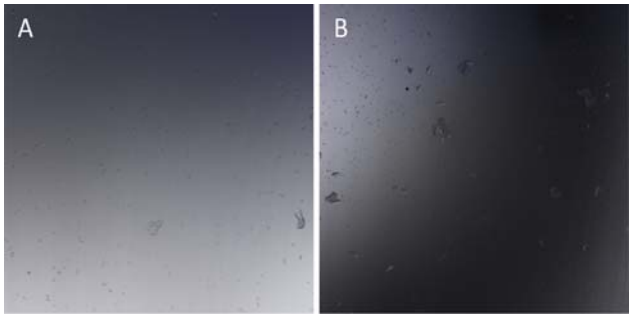

Notes: (A) S. aureus; (B) S. aureus agglutination caused by catesbeianalectin

Fig. 4: S. aureus-agglutinating activity of catesbeianalectin (10 μg/mL)

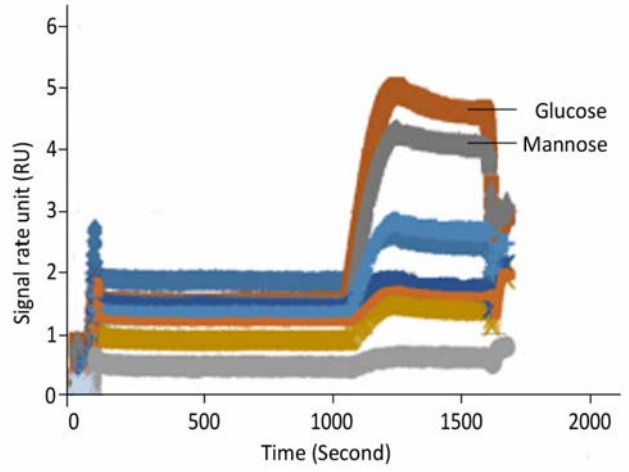

Fig. 5: SPRi detection of ConA

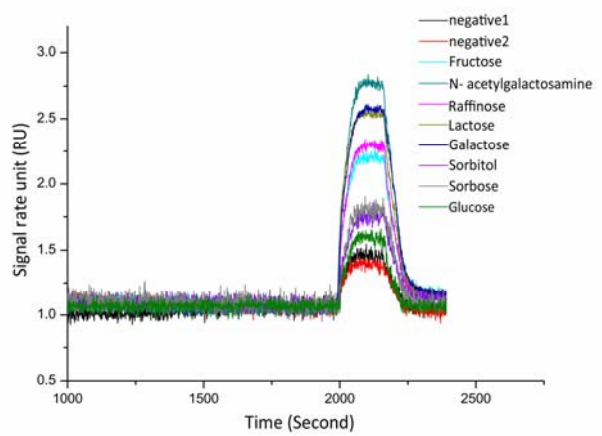

Fig. 6: SPRi detection of catesbeianalectin

^{125}I-catesbeianalectin labeling yield and quality appraisal

Measurement using the radioactive TLC scanner showed that the labeling yield of ^{125}I-catesbeianalectin was 97.3% (fig. 7A). The marker purity after purification was 99.3% (fig. 7B). fig. 7C shows the results of measurements using free ^{125}I TLC scanning.

The radiochemical purity of ^{125}I-catesbeianalectin after 6 h of storage was greater than 90% (fig. 7I). After 6 h of storage mixed with serum, the radiochemical purity of ^{125}I-catesbeianalectin remained at approximately 95%. These results indicate that ^{125}I-labeled catesbeianalectin is stable *in vivo*.

Radioactive in vivo imaging in ICR mice at different time points after administration of ^{125}I-catesbeianalectin

Continuous *in vivo* imaging was used to provide a preliminary understanding of ^{125}I-catesbeianalectin metabolism *in vivo* (fig. 8). In the intravenous administration group, metabolism occurred in 15 min, a radioactive signal was found in the abdominal cavity in 30 min, and metabolism was complete in 6 h. In the intraperitoneal administration group, absorption occurred immediately, while metabolism began within 1 h and was completed in 3-6h. In the intragastric administration group, the drug accumulated in the stomach and was absorbed mainly via this organ; metabolism began in 1.5 h and was basically complete in 6h.

^{125}I-catesbeianalectin distribution in various organs of ICR mice

^{125}I-catesbeianalectin was stable in mouse serum for at least 6 hours (fig. 8I), indicating that it had good stability sufficient for a tracer test. Analysis of changes in radioactive drug concentrations in mouse organs at different time points following different modes of administration resulted in a metabolic curve (fig. 9). Following tail vein injection, ^{125}I-catesbeianalectin was mainly found in the liver, lung, spleen, and stomach; however, the maximum concentration and fastest metabolic rate were found in the liver, while ^{125}I-catesbeianalectin was absorbed less in other organs such as the kidney, heart, and brain, where it was minimally distributed. Following intraperitoneal injection, ^{125}I-catesbeianalectin was mainly found in the spleen and stomach; the peak radioactive drug concentration occurred in the stomach after 2h, whereas ^{125}I-catesbeianalectin was absorbed less in other organs such as the kidney, liver, heart, and lung, and brain, where it was minimally distributed. Following intragastric administration, ^{125}I-catesbeianalectin was mainly found in the stomach, where the maximum radioactive drug concentration was observed; ^{125}I-catesbeianalectin was absorbed less in other organs such as the lung, kidney, and liver and brain, where it was minimally distributed.

DISCUSSION

Lectins bind specifically to carbohydrate structures that vary between organs and tissues; therefore, it may be used

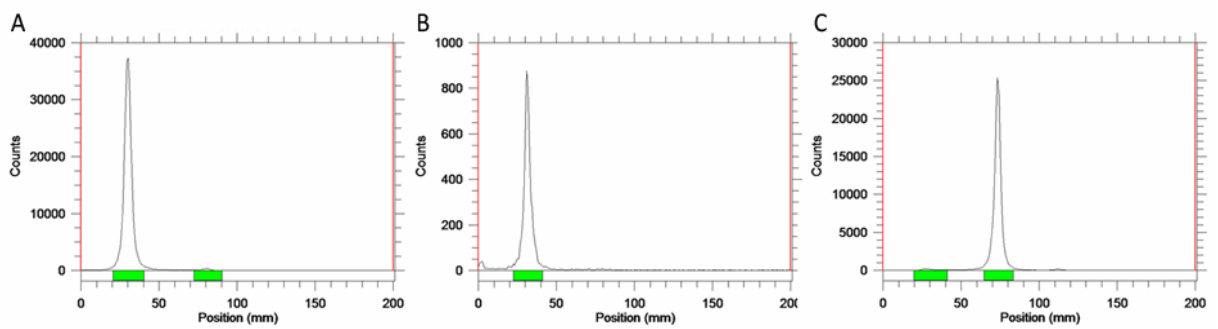

Notes: (A) TLC chromatogram of 125I-catesbeianalectin; (B) TLC chromatogram after purification; (C) TLC chromatogram of the free 125I isotope

Fig. 7 Representative TLC chromatograms of 125I-catesbeianalectin

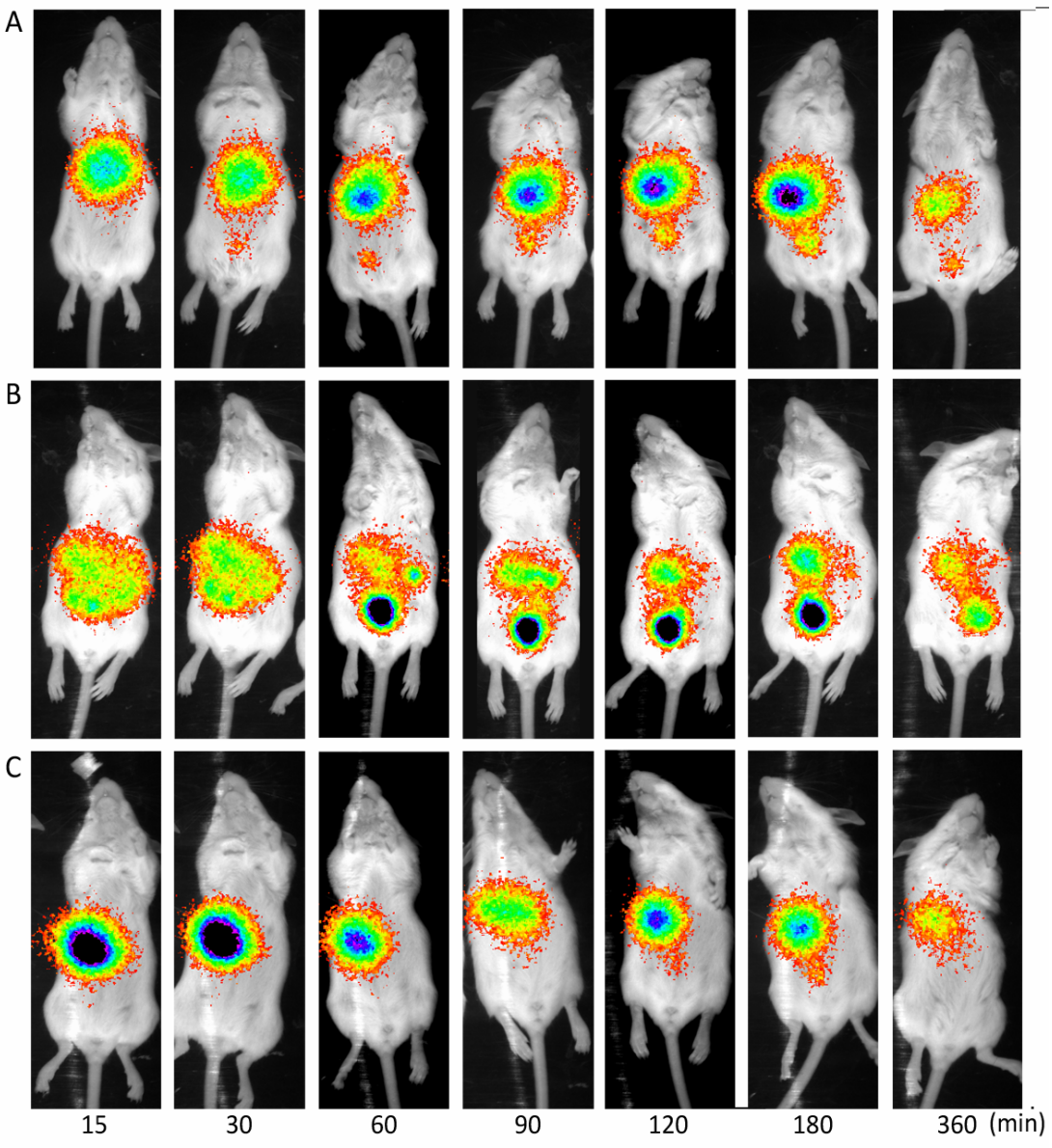

Notes: (A) intravenous injection; (B) intraperitoneal injection; (C) irrigation

Fig. 8: Isotope imaging after three administrations of 125I-catesbeianalectin to mice

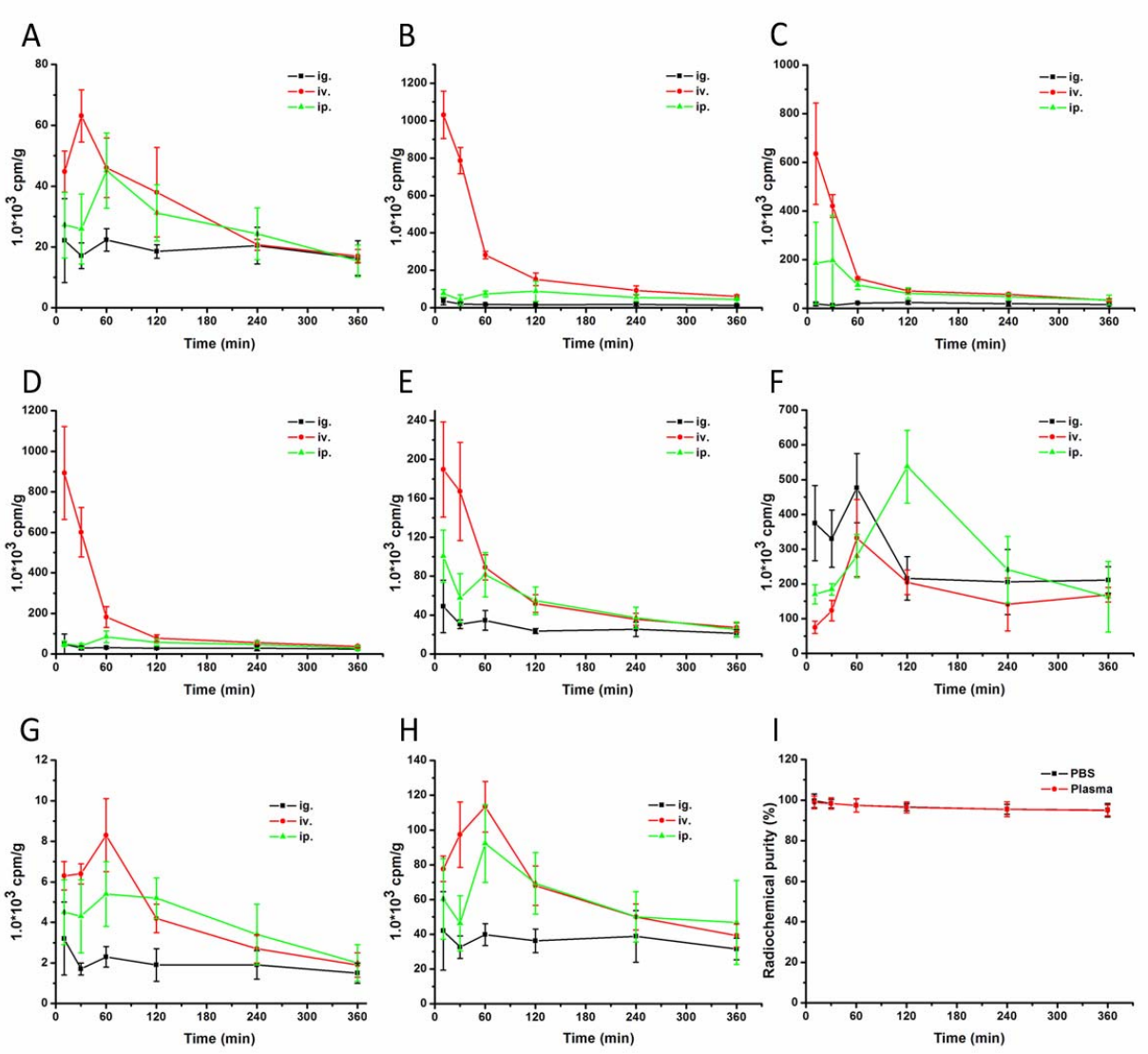

Notes: (A-H) heart, liver, spleen, lung, kidney, stomach, brain, and blood

Fig. 9: Radiocount-time curves of blood and different tissues after intragastric (ig), intravenous (iv), and intraperitoneal (ip) administration to mice (n = 4), as well as the stability of 125I-catesbeianalectin in plasma

as a carrier for targeted drug delivery and has attracted attention from researchers. Decades of effort have been focused on developing a lectin suitable for drug delivery, but most lectins have molecular weight greater than 10 kD, which may lead to serious side effects such as toxicity and strong immunogenicity. However, low-molecular-weight lectins lack many of the defects of high-molecular-weight lectins and represent ideal carriers for targeted drug delivery. Immunogenicity is an important part of biomedical clinical safety evaluation. Drug-induced immune responses influence the dynamics, efficacy, and safety of all drugs (Vasta *et al.,* 2011). This study shows that catesbeianalectin (MW 1.47 kD) at a coating concentration of 80μg/mL has relatively low immunogenicity.

Animal lectins can be divided into C-type lectins, S-type lectins, P-type lectins, I-type lectins, and pentraxins based on carbohydrate recognition domains (CRD) that influence carbohydrate binding activity and conserved amino acid sequences. SPRi showed that catesbeianalectin binds galactose and N-acetylgalactosamine. CD spectrometry showed that catesbeianalectin is an S-type lectin with a PPII-type helical secondary structure. PPII helical structures are found in fiber proteins, folding proteins, and non-folding proteins. Our demonstration of the PPII helix in catesbeianalectin provides a theoretical basis for further *in vivo* studies of the applications of catesbeianalectin.

Radionuclide labeling and tracing techniques are widely used evaluation of drug pharmacokinetics (Ruggiero *et al.,*

Table 1: Determination of the optimal coating concentration and antibody dilutions of OVA

Antigen concentrations (μg/mL)	Serum dilutions											
	1:100			1:200			1:400			1:800		
	P	N	P/N	P	N	P/N	P	N	P/N	P	N	P/N
0.25	1.69	0.051	33.14	0.94	0.048	19.58	0.78	0.061	12.79	0.42	0.053	7.92
0.125	1.54	0.049	31.43	0.67	0.054	12.41	0.63	0.052	12.12	0.31	0.062	5.00
0.06	1.46	0.052	28.08	0.55	0.047	11.70	0.46	0.056	8.21	0.13	0.058	2.24
0.03	1.34	0.053	25.28	0.43	0.049	8.78	0.32	0.045	7.11	0.15	0.059	2.54

Table 2: Determination of the optimal antigen concentration and antibody dilutions of WGA

Antigen concentrations (μg/mL)	Serum dilutions											
	1:400			1:800			1:1600			1:3200		
	P	N	P/N	P	N	P/N	P	N	P/N	P	N	P/N
0.03	2.14	0.062	34.52	1.65	0.053	31.13	1.41	0.048	29.38	0.93	0.066	14.09
0.015	1.63	0.058	28.10	0.94	0.055	17.09	1.30	0.053	24.53	0.68	0.058	11.72
0.008	0.99	0.061	16.23	0.32	0.063	5.08	0.88	0.048	18.33	0.46	0.062	7.42
0.004	0.62	0.054	11.48	0.27	0.049	5.51	0.54	0.064	8.44	0.36	0.051	7.06

Table 3: Determination of the optimal antigen coating concentration and antibody dilutions of catesbeianalectin

Antigen concentrations (μg/mL)	Serum dilutions											
	1:25			1:50			1:100			1:200		
	P	N	P/N	P	N	P/N	P	N	P/N	P	N	P/N
80	0.73	0.053	13.77	0.57	0.055	10.36	0.51	0.046	11.09	0.45	0.066	6.82
40	0.61	0.062	9.84	0.56	0.064	8.75	0.49	0.062	7.90	0.42	0.059	7.12
20	0.43	0.049	8.78	0.41	0.058	7.07	0.40	0.058	6.89	0.33	0.062	5.32
10	0.31	0.048	6.46	0.38	0.047	8.09	0.39	0.053	7.36	0.32	0.051	6.27

P: Positive, N: negative

2010). ^{125}I is widely used because it is economical, easy to use, has a long half-life, and produces reliable labeling results (Yue *et al.,* 2013). The ^{125}I-catesbeianalectin labeling yield was 97.3%, with purity of 99.3% and good stability in mouse serum for at least 6h. Therefore, with its high radiochemical purity and good stability in vitro, ^{125}I-catesbeianalectin is suitable for tracer experiments studying the *in vivo* distribution of catesbeianalectin.

The distribution of ^{125}I-catesbeianalectin in the body reflects the complexity of its *in vivo* absorption and metabolism processes (Li *et al.,* 2008). Following tail vein injection, the concentration of ^{125}I-catesbeianalectin was greatest in the liver, spleen, and lung, but the drug was absent from these organs within 1 h after administration. This phenomenon may have two explanations: 1) ^{125}I-catesbeianalectin may specifically bind with the corresponding organ through some mechanism; 2) catesbeianalectin has a strong hem agglutination effect. With the rich blood supply in the liver, spleen and lungs, ^{125}I-catesbeianalectin bound with red blood cells was destroyed by phagocytic cells. In contrast, following intraperitoneal and intragastric administration, ^{125}I-catesbeianalectin was highly distributed in the stomach and spleen (Zhao *et al.,* 2013). For every tested mode of administration, the radioactive drug concentration was lowest in the brain, indicating that ^{125}I-catesbeianalectin did not pass the blood-brain barrier. Following tail vein injection, ^{125}I-catesbeianalectin was mainly metabolized by the liver. Following intraperitoneal and intragastric administration, ^{125}I-catesbeianalectin was mainly metabolized through the stomach. Tail vein injection seemed to the best route of administration for catesbeianalectin, because ^{125}I-catesbeianalectin administered via this route reached high tissue concentrations and was metabolized rapidly. Dynamic *in vivo* imaging of mice following administration of ^{125}I-catesbeianalectin confirmed the results described above. Taken together, the results of this study provide an empirical basis for further exploration of catesbeianalectin as a targeted drug carrier.

CONCLUSION

We identified a catesbeianalectin via screening a bullfrog skin cDNA library. The catesbeianalectin polypeptide (1.47 kD) is the smallest known lectin in terms of molecular weight. The catesbeianalectin has a PPII helix secondary structure and is an S-type lectin. It able to induce agglutination of rabbit erythrocytes and a variety of pathogens include *Staphylococcus aureus*, *Streptococcus suis* type 2, *Actinobacillus*

pleuropneumoniae, and piglet paratyphoid *Salmonella*. The mean serum titer in catesbeianalectin-immunized Balb/c mice was 1:25, which was significantly lower than that of positive controls immunized with wheat germ agglutinin. ^{125}I-labeled catesbeianalectin did not pass the blood-brain barrier. This study provides a basis for further research on the potential of catesbeianalectin as a carrier in targeted drug delivery.

ACKNOWLEDGEMENTS

This work was supported by the National Natural Science Foundation of China (31201886, 31572492); the General Fund of Application Foundation & Advanced Technology Program, Tianjing, China (14JCYBJC3000); the Veterinary "innovative talent people of young and middle age key members project" of Tianjin, China.

REFERENCES

Gao H, Xiong J, Cheng T, Liu J, Chu L, Liu J, Ma R and Shi L (2013). *In vivo* distribution of mixed shell micelles with tunable hydrophilic/hydrophobic surface. *Biomacromolecules.,* **14**(2): 460-467.

Gao H, Liu J, Yang C, Cheng T, Chu L, Xu H, Meng A, Fan S, Shi L and Liu J (2013). The impact of PEGylation patterns on the *in vivo* biodistribution of mixed shell micelles. *Int. J. Nanomedicine.,* **8**: 4229-4246.

Jemal A, Murray T, Samuels A, Ghafoor A, Ward E and Thun MJ (2003). Cancer statistics. CA. *Cancer J. Clin.,* **53**(1): 25-26.

Jiang L, Peng L, Zhang Y, Chen J, Zhang D and Liang S (2009). Expression, purification and characterization of a group of lectin-like peptides from the spider *Ornithoctonus huwena*. Peptides, **30**(4): 669-674.

Lehr CM (2000). Lectin-mediated drug delivery: the second generation of bioadhesives. *J. Control Release,* **65**(1-2): 19-29.

Lehr CM and Gabor F (2004). Lectins and glycoconjugates in drug delivery and targeting. *Adv. Drug Deliv. Rev.,* **56**(4): 419-420.

Li C, Zhao X, Wang Y, Yang H, Li H, Li H, Tian W, Yang J and Cui J (2013). Prolongation of time interval between doses could eliminate accelerated blood clearance phenomenon induced by pegylated liposomal topotecan. *Int. J. Pharm.,* **443**(1-2): 17-25.

Li J, Wu H, Hong J, Xu X, Yang H, Wu B, Wang Y, Zhu J, Lai R, Jiang X, Lin D, Prescott MC and Rees HH (2008). Odorranalectin is a small peptide lectin with potential for drug delivery and targeting. *PLoS. One,* **3**(6): e2381.

Ruggiero A, Holland JP, Lewis JS and Grimm J (2010). Cerenkov luminescence imaging of medical isotopes. *J. Nucl. Med.,* **51**(7): 1123-1130.

Vasta GR, Nita-Lazar M, Giomarelli B, Ahmed H, Du S, Cammarata M, Parrinello N, Bianchet MA and Amzel LM (2011). Structural and functional diversity of the lectin repertoire in teleost fish: Relevance to innate and adaptive immunity. *Dev. Comp. Immunol.,* **35**(12): 1388-1399.

Yang C, Chu L, Zhang Y, Shi Y, Liu J, Liu Q, Fan S, Yang Z, Ding D, Kong D and Liu J (2015). Dynamic biostability, biodistribution and toxicity of L/D-peptide-based supramolecular nanofibers. *ACS Appl. Mat. Interfaces.,* **7**(4): 2735-2744.

Yue O, Hong SX, Yan J, Chu J and Yan C (2013). Progress in relative quantitative analysis of biological molecules with stable isotope labeling. *Chin. Sci. Bull.,* **58**(27): 2762-2778.

Zhao Q, Yan P, Yin L, Li L, Chen XQ, Ma C and Wang RF (2013). Validation study of I-RRL: Assessment of biodistribution, SPECT imaging and radiation dosimetry in mice. *Mol. Med. Rep.,* **7**(4): 1355-1360.

Zhao R, Han J and Han W (2009). Identification and cloning of two novel temporins from Lithobates catesbeianus. *Prog. Biochem. Biophys.,* **476**(4): 1064-1070.